

# UC San Diego

## UC San Diego Previously Published Works

### Title

Optical Microangiography and Progressive Ganglion Cell-Inner Plexiform Layer Loss in Primary Open-Angle Glaucoma

### Permalink

<https://escholarship.org/uc/item/36q7g63n>

### Authors

Rao, Harsha L  
Dasari, Srilakshmi  
Puttaiah, Narendra K  
[et al.](#)

### Publication Date

2022-06-01

### DOI

10.1016/j.ajo.2021.11.029

Peer reviewed



Published in final edited form as:

*Am J Ophthalmol.* 2022 June ; 238: 36–44. doi:10.1016/j.ajo.2021.11.029.

## Optical microangiography and progressive ganglion cell-inner plexiform layer loss in primary open angle glaucoma

Harsha L Rao<sup>1,2</sup>, Srilakshmi Dasari<sup>1</sup>, Narendra K Puttaiah<sup>1</sup>, Zia S Pradhan<sup>3</sup>, Sasan Moghimi<sup>4</sup>, Kaweh Mansouri<sup>5,6</sup>, Carroll AB Webers<sup>2</sup>, Robert N Weinreb<sup>4</sup>

<sup>1</sup>Narayana Nethralaya, 63, Bannerghatta Road, Hulimavu, Bangalore 560076, India.

<sup>2</sup>University Eye Clinic Maastricht, University Medical Center, Maastricht, the Netherlands.

<sup>3</sup>Narayana Nethralaya, 121/C, Chord Road, Rajajinagar, Bangalore 560010, India.

<sup>4</sup>Hamilton Glaucoma Center, Shiley Eye Institute, and Viterbi Family Department of Ophthalmology, University of California San Diego, La Jolla, CA, United States.

<sup>5</sup>Glaucoma Research Center, Montchoisi Clinic, Swiss Visio, Lausanne, Switzerland.

<sup>6</sup>Department of Ophthalmology, University of Colorado, Denver, CO, United States.

### Abstract

**Purpose:** To evaluate the association between optical microangiography (OMAG) measurements and progressive ganglion cell-inner plexiform layer (GCIPL) loss in primary open angle glaucoma (POAG).

**Design:** Prospective case-series

**Methods:** Sixty-three eyes of 38 POAG patients were studied for at least 2 years and with at least 3 optical coherence tomography (OCT) examinations. Only those hemifields with mild to moderate functional damage at baseline (106 hemifields) were included in the analysis. OMAG imaging was performed at the baseline visit. Effect of clinical parameters (age, gender, central corneal thickness, presence of disc hemorrhage, mean and fluctuation of intraocular pressure), baseline mean deviation (MD), retinal nerve fiber layer (RNFL) and ganglion cell inner plexiform layer (GCIPL) thickness and baseline OMAG measurements (peripapillary and macular perfusion density [PD] and vessel density [VD]) on the rate of change of GCIPL thickness was evaluated using linear mixed models.

**Results:** Average ( $\pm$  standard deviation) MD, quadrant RNFL and sector GCIPL thickness of the analyzed hemifields respectively at baseline were  $-5.2 \pm 2.8$  dB,  $94.5 \pm 20.0$   $\mu$ m, and  $72.4 \pm 8.7$   $\mu$ m respectively. Peripapillary PD and VD in the quadrant were  $43.1 \pm 7.0\%$  and  $17.0 \pm 2.6$  mm/mm<sup>2</sup> respectively. Macular PD and VD in the quadrant were  $37.2 \pm 6.9\%$  and  $15.1 \pm 2.6$  mm/mm<sup>2</sup>

**Corresponding author:** Harsha L Rao, Narayana Nethralaya, 63, Bannerghatta Road, Hulimavu, Bangalore 560076, India. Ph: +91-80-62221449, Fax: +91-80-23377329, harshalaxmanarao@gmail.com.

**Contributions of Authors:** Design and conduct of study: all authors; Collection, management, analysis, and interpretation of the data: all authors; preparation, review, or approval of the manuscript: all authors.

**Financial disclosures:** Rao HL: Santen (C), Allergan (C); Dasari S: none; Puttaiah NK: none; Pradhan ZS: none; Moghimi S: none; Mansouri K: Santen (C), Allergan (S), ImplanData (C); Webers CAB: Alcon (S), Allergan (C), Pfizer (C), Santen (C); Weinreb RN: Optovue (S), Meditec-Zeiss (S), Heidelberg Engineering (S), Allergan (C), Centervue (S), ImplanData (C), Equinox (C), Topcon (C).

respectively. Rate of sector GCIPL change was  $-0.97 \pm 0.15$   $\mu\text{m}/\text{year}$ . Multivariate mixed models showed that lower peripapillary PD (coefficient: 0.04,  $p=0.01$ ) and VD (coefficient: 0.09,  $p=0.05$ ) were significantly associated with faster rate of GCIPL loss.

**Conclusions:** Lower baseline peripapillary OMAG measurements were significantly associated with a faster rate of GCIPL loss in mild to moderate POAG.

---

## INTRODUCTION

Optical coherence tomography (OCT) angiography is a relatively recent, non-invasive, dye-less technology which enables visualization of the blood vessels of the optic nerve head (ONH) and retina.<sup>1</sup> OCT angiography (OCTA) achieves blood vessel visualization by using software algorithms that analyze the variation in the OCT signal caused by moving particles within the vessels, such as red blood cells.<sup>1</sup> There are several different algorithms that are commercially available for OCTA including split spectrum amplitude-decorrelation angiography (SSADA, RTVue-XR SD-OCT, Optovue Inc., Fremont, CA),<sup>2, 3</sup> OCTA ratio analysis (OCTARA, DRI OCT Triton, Topcon, Japan)<sup>4</sup> and optical microangiography (OMAG, Cirrus HD-OCT, Carl Zeiss Meditec Inc., Dublin, CA).<sup>5-7</sup> Irrespective of the type of algorithm applied, one prominent OCTA feature in eyes with glaucoma is the reduction of superficial vessels in the peripapillary and macular regions.<sup>2, 8-11</sup> A few studies have evaluated the association between baseline superficial vascular parameters measured using OCTA and the risk of primary open angle glaucoma (POAG) progression.<sup>12-16</sup> Some studies found no association between the density of superficial vessels at baseline, and visual field (VF) progression.<sup>13, 14</sup> Results of studies evaluating the association between baseline OCTA parameters and progressive retinal nerve fiber layer (RNFL) thinning have been contradictory. Although lower densities of superficial vessels in the peripapillary<sup>12, 16</sup> and macular<sup>12</sup> regions were found to be associated with faster RNFL thinning in few studies, others found no association between these parameters.<sup>13-15</sup> The difference in these study results can have several possible explanations, including the use of different OCTA algorithms to delineate the retinal vasculature. While most of the studies used the SSADA algorithm,<sup>12, 13, 15</sup> one study used OCTA ratio analysis<sup>14</sup> and another used optical microangiography.<sup>16</sup>

There only have been few reports describing the association between OCTA parameters and progressive macular inner retinal (ganglion cell-inner plexiform layer, GCIPL) thinning. Two studies, one using SSADA and another used the OCTARA algorithm, found no association between superficial macular vessel density and progressive GCIPL thinning.<sup>14, 15</sup> However, the utility of OMAG measurements in predicting progressive GCIPL thinning in POAG previously has not been described. The purpose of the present study was to evaluate the association between baseline OMAG measurements and progressive GCIPL loss in POAG patients.

## METHODS

This report was an analysis of participants included in a prospective longitudinal study designed to evaluate optic nerve structure, vasculature and visual function in glaucoma (Narayana Nethralaya Glaucoma Progression Study, NNGPS) conducted at Narayana

Nethralaya, a tertiary eye care center in Bengaluru, South India. The detailed methodology of NNGPS has been described earlier.<sup>16</sup> Participants in NNGPS include normal subjects, patients with different subtypes of glaucoma and glaucoma suspects, who are serially evaluated clinically and with functional and imaging tests every 6 to 12 months. All participants from the study who met the inclusion criteria described below were enrolled in the current report. The methodology adhered to the tenets of the Declaration of Helsinki for research involving human subjects. Written informed consent was obtained from all participants and the study was approved by the Ethics Committee of Narayana Nethralaya.

Baseline and follow-up examinations consisted of a comprehensive eye examination (including review of medical history, best-corrected visual acuity (BCVA), slit-lamp biomicroscopy, Goldmann applanation tonometry, gonioscopy, and dilated fundus examination using a 90-diopter (D) lens), stereoscopic optic disc photography, OCT imaging with Cirrus HD-OCT (model 5000), and visual field (VF) examination with standard automated perimetry.

Inclusion criteria for all participants were age  $\geq 18$  years, corrected distance visual acuity of 20/40 or better and refractive error within  $\pm 5$  D sphere and  $\pm 3$  D cylinder. Exclusion criteria were presence of any media opacities that prevented good quality OCT and OCTA scans, or any retinal or neurological disease (other than glaucoma) which could confound the evaluation. For the current study, only those POAG patients with at least 2 years of follow-up and a minimum of 3 HD-OCT scanning sessions were included. Eyes were classified as having glaucoma if they showed characteristic glaucomatous VF damage and optic disc changes (defined below). Eyes that underwent any intraocular surgery during the follow-up (cataract, glaucoma or combined cataract and glaucoma surgery) were excluded from the analysis.

All participants underwent a baseline VF examination using the Humphrey Field analyzer 3 (model 860, Carl Zeiss Meditec Inc., Dublin, CA), and the Swedish interactive threshold algorithm (SITA) standard 24-2 program was performed. VFs were considered reliable if the fixation losses were less than 20%, and the false positive and false negative response rates were less than 15%. The VF was considered glaucomatous if the glaucoma hemifield test result was outside normal limits, pattern standard deviation was abnormal at  $p < 5\%$  level, or  $\geq 3$  test points in a cluster on pattern deviation probability plot were abnormal at  $p < 5\%$  with at least one point abnormal at  $p < 1\%$ . Visual sensitivity loss quantified by mean deviation (MD) was used to determine the severity of functional damage. In addition to the overall MD of the field, MD of both the superior and inferior hemifields as provided on the Glaucoma Workplace (software version 3.5, Carl Zeiss Meditec Inc., Dublin, CA) were used in the current analysis. Superior and inferior VF hemifields were evaluated separately for inclusion and VF hemifields with MD worse than  $-12$  dB were excluded to ensure the ability to detect progressive GCIPL thinning without reaching the measurement floor.

OCT scanning was performed using the optic disc cube  $200 \times 200$  and macula cube  $200 \times 200$  scan protocols. From the optic disc cube scans, RNFL thickness was calculated along a circle 3.46 mm in diameter positioned evenly around the center of the optic disc. Average RNFL thickness over the entire circle as well as the 4 quadrants (temporal, superior, nasal

and inferior) of 90 degrees each were determined. In the current study, RNFL thickness in the superior and inferior 90 degree quadrants were analyzed. From the macula cube scans, GCIPL thickness measurements were calculated within a 14.13-mm<sup>2</sup> elliptical annulus centered on the fovea with an inner vertical radius of 0.5 mm and outer vertical radius of 2 mm, stretched horizontally by 20%. The thickness parameters derived from the macula scan were the average GCIPL thickness across the entire elliptical annulus and the thickness at six 60-degree sectors (superior, supero-nasal, infero-nasal, inferior, infero-temporal, and supero-temporal) of the elliptical annulus. In the current study, GCIPL thickness in the superior and inferior 60-degree sectors alone were used for analysis as these are the sectors analyzed in the trend-based progression reports on the Glaucoma Workplace. Also, these are the sectors that closely correspond to the superior and inferior quadrant of the macular OMAG scans used in the current study (described below).

OCTA of the peripapillary region and the macula was performed by trained technicians at the baseline visit using Cirrus HD-OCT (software version 10.0.0.14618). The procedure of OCTA imaging with Cirrus HD-OCT has been detailed previously.<sup>7, 16–18</sup> The algorithm used to achieve blood vessel delineation on Cirrus HD-OCT is the optical microangiography (OMAG).<sup>6</sup> OMAG utilizes both the intensity and phase information from B scans repeated at the same position to delineate blood vessels.<sup>7</sup> The peripapillary and macular regions were imaged using a 6×6 mm cube scan centered on the optic disc and the fovea respectively as described previously.<sup>17, 18</sup> The 6×6 mm scan pattern has 350 A-scans in each B-scan along both the horizontal and the vertical directions. Each B-scan is repeated 2 times in the 6×6 mm scan. The manufacturer's retinal tracking technology was used to reduce motion artifacts. From the volume scans, retina and choroid were segmented into multiple slabs and 2-dimensional angiographic images of each slab were generated. In the current study, angiographic images of the superficial peripapillary and superficial macular slabs were analyzed. The inner boundary of the superficial retinal slab is the internal limiting membrane (ILM) and the outer boundary is the inner plexiform layer (IPL). Angiometric software of the Cirrus HD-OCT automatically calculates 2 parameters from the superficial retinal layer slab, namely perfusion density (PD) and vessel density (VD) and perfusion density (PD). PD is defined as the total area of perfused vasculature per unit area in the region of measurement (measured as %). VD is defined as the total length of perfused vasculature per unit area in the region of measurement (measured as mm/mm<sup>2</sup>). The angiometric software, primarily designed to be used at the macula, calculates the vessel and perfusion density parameters in the various sectors of the Early Treatment Diabetic Retinopathy Study (ETDRS) grid placed over the macula (Figure 1a). The same grid was placed on the peripapillary scan and manually centered on the optic disc as shown in Figure 1b. Angiometric parameters measured on the 4 outer sectors of the grid, i.e., between the outer 2 circles (temporal, superior, nasal and inferior sectors), were determined. In the current study, the OMAG measurements from the superior and inferior outer quadrants (each of 90 degree) of the baseline peripapillary and macular scans were analyzed.

The dependent variable in the current analysis was the rate of change of GCIPL thickness over time (defined in the statistical analysis section) measured on the serial macular cube scans. The follow-up macular cube scans were referenced to the baseline scan using the manufacturer's "track to prior scan" option from the time this feature was available.<sup>19</sup>

When the “track to prior scan” option is selected, the previously saved scanning laser ophthalmoscopy (SLO) fundus image of the baseline scan is overlaid in the scan pattern box over the live SLO fundus image matching for the blood vessel branchings; this allows the repeat scans to be tracked and acquired exactly on the baseline scan.

All the baseline examinations for a particular subject were performed on the same day. Image quality was assessed for all OCT and OMAG scans. Poor quality images, defined as those with a signal strength less than 6, and images with motion artifacts and segmentation errors were excluded from the analysis. Additionally, OMAG images with poor clarity or local weak signal were also excluded.

## STATISTICAL ANALYSIS

Descriptive statistics included mean and standard deviation for continuous variables and percentages for categorical variables. The effect of clinical, VF, OCT and OMAG parameters on rate of change of sector GCIPL thickness (GCIPL slope) was evaluated using multilevel linear mixed models with random intercepts and random slopes.<sup>20, 21</sup> In this multilevel model, GCIPL sector (level 1) was nested within eye (level 2) and the eye was nested within subject (level 3). The change in the outcome variable (sector GCIPL thickness) was explored using a linear function of time, and random intercepts and random slopes introduced patient-, eye- and quadrant-specific deviations from the average value. The model accounts for the fact that different sectors and eyes can have different GCIPL slopes over the follow-up period, while accommodating correlations between the two sectors and/or both eyes of the same individual because of the nested design.<sup>20, 21</sup> Because the rate of GCIPL change may depend on the disease severity, an unstructured covariance between random effects was assumed, allowing for correlation between intercepts and slopes.<sup>22</sup> Effects of predictor variables were assessed on the baseline sector GCIPL thickness (baseline severity), and on the change in GCIPL thickness over time by introducing interaction terms between time and predictor variables. The clinical parameters (predictors) investigated for their association with baseline GCIPL thickness and rate of GCIPL thickness change were the age, gender, presence of hypertension, diabetes, central corneal thickness (CCT), presence of DH, follow-up duration, mean IOP and the fluctuation (standard deviation) of IOP during the follow-up. The baseline VF, OCT and OMAG predictors investigated were the hemifield MD, sector GCIPL thickness, quadrant RNFL thickness, peripapillary PD and VD, and macular PD and VD. Univariate models were constructed containing one predictor along with its interaction with time. Predictors associated with the rate of GCIPL change at  $P < 0.10$  in univariate analysis were introduced into multivariate analysis. Collinearity between predictor variables were evaluated and predictors which correlated with each other (correlation coefficient of  $> 0.60$ ) were evaluated in separate multivariate models. Rates of sector GCIPL change were obtained from the linear mixed models using best linear unbiased prediction (BLUP).<sup>23, 24</sup> Statistical analyses were performed using Stata software version 14.2 (StataCorp, College Station, TX). A  $p$  value of 0.05 was considered statistically significant for the final analysis.

## RESULTS

One hundred and six VF hemifields with mild to moderate functional loss from 63 eyes of 38 POAG patients were included in the study. Table 1 shows the baseline clinical, VF, OCT, OMAG features of the included patients. Table 1 also shows the mean and fluctuation of IOP during the follow-up duration. Mean follow-up duration was  $3.0 \pm 0.8$  years and mean number of OCT examinations performed during the follow-up was  $4.1 \pm 1.1$  (range 3–7). Mean number of anti-glaucoma medications at baseline was  $1.2 \pm 0.7$ . One eye had poor quality optic disc OMAG scan, 10 eyes had poor quality macular OMAG scans and 3 eyes had poor quality both on disc and macular OMAG scans. OMAG data of these eyes were excluded while the rest of the data from these eyes were used for the analysis. DH during the follow-up duration was noted in 6 quadrants of 6 eyes (1 superior and 5 inferior quadrant). The lens was clear at the baseline visit in 36 eyes, pseudophakic in 7 eyes and showed early cataractous changes (peripheral cortical changes, nuclear sclerosis grade 1) in 20 eyes. Rate of change of GCIPL thickness (GCIPL slope) was  $-0.97 \pm 0.15 \mu\text{m}/\text{year}$  ( $p < 0.001$ ). Rate of GCIPL change in the superior sector was  $-0.90 \mu\text{m}/\text{year}$  (95% CI:  $-1.26$  to  $-0.54$ ) and that in the inferior sector was  $-1.03 \mu\text{m}/\text{year}$  (95% CI:  $-1.39$  to  $-0.67$ ).

Table 2 shows the effect of each predictor on the baseline GCIPL thickness in univariate analysis. Thinner baseline GCIPL value (greater severity of disease) was significantly associated with lower spherical equivalent refraction (more myopic), lower MD, thinner RNFL, and lower OMAG measurements. Table 2 also shows the effect of each predictor on the sector GCIPL slope. Faster rate of GCIPL loss (more negative slope) was associated with greater age (coefficient =  $-0.03$ ,  $p = 0.02$ ), female gender (coefficient =  $-0.77$ ,  $p = 0.05$ ), presence of disc hemorrhage (coefficient =  $-0.93$ ,  $p = 0.03$ ), lower peripapillary PD (coefficient =  $0.04$ ,  $p = 0.01$ , Figure 2a) and lower peripapillary VD (coefficient =  $0.09$ ,  $p = 0.04$ , Figure 2b). GCIPL slope was not significantly associated with either the baseline MD, RNFL thickness, GCIPL thickness, macular OMAG measurements, central corneal thickness, or the IOP parameters. GCIPL slope was also not associated with changes in the signal strength of the follow-up macular cube scans.

Table 3 shows the results of multivariate models incorporating the factors found to be significantly associated with rate of GCIPL change in univariate analysis. As collinearity was noted between peripapillary PD and VD (correlation coefficient =  $0.98$ ,  $p < 0.001$ ), separate multivariate models were built incorporating each of them with the other predictors found to be significantly associated with rate of GCIPL change on univariate analysis. A 1% lower peripapillary PD at baseline was associated with a  $0.04 \mu\text{m}/\text{year}$  faster rate of GCIPL loss ( $p = 0.01$ ) in the corresponding sector. Similarly, a  $1\text{mm}/\text{mm}^2$  lower peripapillary VD at baseline was associated with a  $0.09 \mu\text{m}/\text{year}$  faster rate of GCIPL loss ( $p = 0.05$ ) in the corresponding sector. Figure 3 is an example of an eye showing baseline peripapillary and macular OMAG and OCT scans (a-d) along with GCIPL changes in superior and inferior sectors during the follow-up (e-h).

Multivariate models including age, mean IOP during follow-up, presence of DH, CCT and baseline MD in addition to OMAG parameters were also constructed, as these factors have been reported to be associated with glaucoma progression in previous studies. The results

showed that older age (coefficient=-0.03, p=0.01), occurrence of DH (coefficient=-0.77, p=0.02), baseline peripapillary PD (coefficient=0.04, p=0.02) and VD (coefficient=0.08, p=0.06) were associated with the GCIPL slope.

## DISCUSSION

In the current study, baseline peripapillary OMAG parameters were significantly associated with progressive GCIPL loss in POAG patients with mild to moderate severity of functional damage. A 1% lower quadrant peripapillary PD at baseline was associated with a 0.04  $\mu\text{m}/\text{year}$  faster rate of GCIPL loss (p=0.01) in the corresponding sector. Similarly, a 1  $\text{mm}/\text{mm}^2$  lower peripapillary VD at baseline was associated with a 0.09  $\mu\text{m}/\text{year}$  faster GCIPL thinning (p=0.05) in the corresponding sector. Macular OMAG measurements at baseline were not associated with GCIPL thinning.

Association between baseline OCTA measurements and progressive GCIPL loss has been evaluated previously in two studies.<sup>14, 15</sup> Li et al evaluated the association between baseline OCTA parameters and GCIPL progression in a Chinese population over a mean follow-up of 29.39 months.<sup>14</sup> The OCTA algorithm used was OCTA ratio analysis, an algorithm which uses the full spectrum of the OCT signal for blood vessel delineation. GCIPL progression was a binary variable defined as the presence of a negative GCIPL slope with p value <5%.<sup>14</sup> They found that a larger foveal avascular zone (FAZ) area was significantly associated with GCIPL progression. Superficial capillary densities (without large vessels) in the peripapillary and macular area were not significantly associated with GCIPL progression.<sup>14</sup> The differences in the results between this and the current study may be due to the differences in the characteristics of the subjects (disease characteristics and ethnicity), OCTA algorithm or the definition of the outcome variable. In another study, Ye et al evaluated the association between GCIPL loss and macular OCTA parameters over a mean follow-up period of 36.6 months.<sup>15</sup> Macular OCTA was performed using 3 mm x 3 mm scan with the SSADA algorithm. Peripapillary OCTA was not performed in this study. Similar to the results of the current study, Ye et al too found that the baseline macular vessel density (vessel density on the OCTA device using the SSADA algorithm was similar to PD on OMAG) was not associated with progressive GCIPL loss (coefficient: 0.0002, p=0.77) when assessed using linear mixed models. While the current study included eyes with mild to moderate glaucoma, both the above studies by Li et al and Ye et al included eyes with advanced severity of glaucoma (MD worse than -12 dB), as well. It is known that the structural measurements of OCT show a floor effect in advanced glaucoma, although to a larger extent with RNFL than GCIPL thickness,<sup>25-28</sup> and therefore are less likely to show further worsening even in progressing eyes.<sup>29</sup> In the current study, glaucoma severity was additionally evaluated hemifield-wise and the hemifields with MD worse than -12 dB were excluded.

A plausible reason for the association between lower OMAG measurements and faster GCIPL loss is the possibility of more rapid retinal ganglion cell (RGC) death in eyes with lower OMAG measurements. Alternatively, it may be due to the existence of dysfunctional RGCs that have lower metabolic demand causing reduction in OMAG measurements.<sup>12</sup> Strangely, the current study found that a faster GCIPL loss was associated with lower



baseline peripapillary OMAG measurements, but not with macular OMAG measurements. We speculate that the reduction of peripapillary microvasculature is more specific than macular microvasculature in glaucoma and that the macular OCTA changes do not provide information about the risk of glaucoma progression. This may be particularly relevant to the Indian population as cross-sectional studies have shown that macular OCTA measurements have a poor ability to differentiate glaucoma from control eyes.<sup>18, 30</sup> Future studies should evaluate if these findings are reproducible in different ethnic populations and when assessed over longer follow-up durations.

Identification of glaucoma patients at risk of progression is useful in planning effective management. Rate of macular inner retinal thickness (GCIPL and ganglion cell complex, GCC) change is a commonly used structural measure of glaucoma progression.<sup>25, 27, 28, 31–34</sup> Progressive macular inner retinal thickness loss is associated with concurrent and subsequent VF progression.<sup>27, 33, 35–37</sup> The slope of GCIPL thickness found in the present study was  $-0.97 \mu\text{m}/\text{year}$ . Most of the previous studies using SDOCT have reported the slope of overall average, superior and inferior sector GCIPL thickness loss in glaucoma patients to be between  $-0.5$  to  $-1 \mu\text{m}/\text{year}$ .<sup>25, 27, 28, 32, 34, 38</sup>

The other baseline factors significantly associated with progressive GCIPL loss in the current study on univariate model were older age, female gender and the occurrence of disc hemorrhage. Previous studies have also found a significant positive association of glaucoma progression with older age and disc hemorrhage.<sup>12, 14, 39–45</sup>

Progressive GCIPL loss in the current study was not associated with the traditional measures of disease severity at baseline (MD, RNFL thickness or the GCIPL thickness). While a few previous studies have found an association between GCIPL loss and measures of disease severity at baseline,<sup>14, 15, 38</sup> few others have found no association between the two.<sup>32, 35</sup> Progressive GCIPL loss in the current study was also not associated with mean IOP, IOP fluctuation or CCT. Each of these clinical factors has been reported to be associated with glaucoma progression in a few previous studies.<sup>13, 38–42, 44–48</sup> As discussed earlier, the differences in the results of these studies may be due to the differences in the characteristics of the subjects, length of follow-up or the definition of the outcome variable. GCIPL loss in the current study was also not associated with the signal strength of the OCT scan similar to that reported in a previous study.<sup>15</sup>

The current study has a few limitations. Although appropriate statistical methods were used for the analysis, progression rates of the 2 sectors of the same eye and two eyes of the same patient could be correlated beyond statistical adjustments. Also, some of the parameters evaluated for their association with progressive GCIPL loss are common to quadrants (like IOP and CCT of the same eye) and eyes (like age and gender of the patient), and can be beyond statistical adjustments. This may be a reason that some of these parameters, which have been shown to be associated with glaucoma progression in previous studies, were not statistically significantly associated with GCIPL loss in the current study. Another limitation is that the area of VF ( $180^\circ$ ), RNFL quadrant ( $90^\circ$ ), OCTA quadrant ( $90^\circ$ ) and GCIPL sector ( $60^\circ$ ) used for the analysis in the current study were not exactly similar topographically. This may also be a reason for not finding an association between measures

of disease severity at baseline and GCIPL loss. However, the regions considered here are the ones topographically closest to each other which are automatically reported by the Cirrus-HDOCT device. Analyzing these regions can help the clinicians better interpret the output provided by the instrument. Another limitation is that a minimum of 3 OCT examinations performed over a follow-up period of at least 2 years were used for the detection of the GCIPL slope. A larger number of OCT examinations and longer duration of follow-up may have provided a more robust estimate of GCIPL change. Also, the interval between OCT exams was not uniform. These may have affected the accuracy and precision of the GCIPL slope estimation. However, GCIPL slope in the current study was estimated using BLUP instead of the ordinary least square (OLS) regression. BLUPs are shrinkage estimates that take into account the results obtained by evaluating the whole sample of eyes.<sup>23</sup> BLUPs give less weight to estimates obtained from eyes with fewer measurements and/or large intra-individual variability and have been shown to be more precise than OLS estimates in such situations.<sup>24</sup> Therefore, the results of the study are less likely to be biased by the limited number and variable intervals between OCT examinations.

In conclusion, lower baseline peripapillary, but not macular, perfusion and vessel density measured using OMAG were significantly associated with a faster rate of GCIPL loss in POAG patients with mild to moderate severity of functional damage. Therefore, OMAG imaging may provide useful information about the risk of glaucoma progression and the rate of disease worsening.

## ACKNOWLEDGEMENTS

### Funding:

supported in part by R01 EY029058 (RNW) from the National Eye Institute and an unrestricted grant from Research to Prevent Blindness (NY, New York)

## REFERENCES

1. Kashani AH, Chen CL, Gahm JK, et al. Optical coherence tomography angiography: A comprehensive review of current methods and clinical applications. *Prog Retin Eye Res* 2017;60:66–100. [PubMed: 28760677]
2. Jia Y, Morrison JC, Tokayer J, et al. Quantitative OCT angiography of optic nerve head blood flow. *Biomed Opt Express* 2012;3:3127–37. [PubMed: 23243564]
3. Jia Y, Tan O, Tokayer J, et al. Split-spectrum amplitude-decorrelation angiography with optical coherence tomography. *Opt Express* 2012;20:4710–25. [PubMed: 22418228]
4. Stanga PE, Tsamis E, Papayannis A, et al. Swept-Source Optical Coherence Tomography Angio (Topcon Corp, Japan): Technology Review. *Dev Ophthalmol* 2016;56:13–7. [PubMed: 27023108]
5. Wang RK, An L, Francis P, Wilson DJ. Depth-resolved imaging of capillary networks in retina and choroid using ultrahigh sensitive optical microangiography. *Opt Lett* 2010;35:1467–9. [PubMed: 20436605]
6. An L, Johnstone M, Wang RK. Optical microangiography provides correlation between microstructure and microvasculature of optic nerve head in human subjects. *J Biomed Opt* 2012;17:116018. [PubMed: 23128971]
7. Rosenfeld PJ, Durbin MK, Roisman L, et al. ZEISS Angioplex Spectral Domain Optical Coherence Tomography Angiography: Technical Aspects. *Dev Ophthalmol* 2016;56:18–29. [PubMed: 27023249]
8. Jia Y, Wei E, Wang X, et al. Optical coherence tomography angiography of optic disc perfusion in glaucoma. *Ophthalmology* 2014;121:1322–32. [PubMed: 24629312]

9. Wang X, Jiang C, Ko T, et al. Correlation between optic disc perfusion and glaucomatous severity in patients with open-angle glaucoma: an optical coherence tomography angiography study. *Graefes Arch Clin Exp Ophthalmol* 2015;253:1557–64. [PubMed: 26255817]
10. Liu L, Jia Y, Takusagawa HL, et al. Optical Coherence Tomography Angiography of the Peripapillary Retina in Glaucoma. *JAMA Ophthalmol* 2015;133:1045–52. [PubMed: 26203793]
11. Yarmohammadi A, Zangwill LM, Diniz-Filho A, et al. Optical Coherence Tomography Angiography Vessel Density in Healthy, Glaucoma Suspect, and Glaucoma Eyes. *Invest Ophthalmol Vis Sci* 2016;57:OCT451–9.
12. Moghimi S, Zangwill LM, Penteadó RC, et al. Macular and Optic Nerve Head Vessel Density and Progressive Retinal Nerve Fiber Layer Loss in Glaucoma. *Ophthalmology* 2018;125:1720–8. [PubMed: 29907322]
13. Shin JW, Song MK, Kook MS. Association Between Progressive Retinal Capillary Density Loss and Visual Field Progression in Open-Angle Glaucoma Patients According to Disease Stage. *Am J Ophthalmol* 2021;226:137–47. [PubMed: 33524366]
14. Li F, Lin F, Gao K, et al. Association of foveal avascular zone area with structural and functional progression in glaucoma patients. *Br J Ophthalmol* 2021 (In Press).
15. Ye C, Wang X, Yu MC, et al. Progression of Macular Vessel Density in Primary Open-Angle Glaucoma: A Longitudinal Study. *Am J Ophthalmol* 2021;223:259–66. [PubMed: 33351744]
16. Rao HL, Dasari S, Puttaiah NK, et al. Optical microangiography and progressive retinal nerve fiber layer loss in primary open angle glaucoma. *Am J Ophthalmol* 2021;233:171–9. [PubMed: 34320375]
17. Rao HL, Dasari S, Riyazuddin M, et al. Diagnostic Ability and Structure-function Relationship of Peripapillary Optical Microangiography Measurements in Glaucoma. *J Glaucoma* 2018;27:219–26. [PubMed: 29329139]
18. Rao HL, Riyazuddin M, Dasari S, et al. Diagnostic Abilities of the Optical Microangiography Parameters of the 3×3 mm and 6×6 mm Macular Scans in Glaucoma. *J Glaucoma* 2018;27:496–503. [PubMed: 29578891]
19. Rao HL, Dasari S, Riyazuddin M, et al. Referenced scans improve the repeatability of optical coherence tomography angiography measurements in normal and glaucoma eyes. *Br J Ophthalmol* 2021;105:1542–7. [PubMed: 32962991]
20. Laird NM, Ware JH. Random-effects models for longitudinal data. *Biometrics* 1982;38:963–74. [PubMed: 7168798]
21. Laird NM, Donnelly C, Ware JH. Longitudinal studies with continuous responses. *Stat Methods Med Res* 1992;1:225–47. [PubMed: 1341659]
22. Medeiros FA, Meira-Freitas D, Lisboa R, et al. Corneal hysteresis as a risk factor for glaucoma progression: a prospective longitudinal study. *Ophthalmology* 2013;120:1533–40. [PubMed: 23642371]
23. Robinson GK. That BLUP is a good thing: the estimation of random effects. *Stat Sci* 1991;6:15–51.
24. Beckett LA, Tancredi DJ, Wilson RS. Multivariate longitudinal models for complex change processes. *Stat Med* 2004;23:231–9. [PubMed: 14716725]
25. Hammel N, Belghith A, Weinreb RN, et al. Comparing the Rates of Retinal Nerve Fiber Layer and Ganglion Cell-Inner Plexiform Layer Loss in Healthy Eyes and in Glaucoma Eyes. *Am J Ophthalmol* 2017;178:38–50. [PubMed: 28315655]
26. Belghith A, Medeiros FA, Bowd C, et al. Structural Change Can Be Detected in Advanced-Glaucoma Eyes. *Invest Ophthalmol Vis Sci* 2016;57:OCT511–8. [PubMed: 27454660]
27. Shin JW, Sung KR, Lee GC, et al. Ganglion Cell-Inner Plexiform Layer Change Detected by Optical Coherence Tomography Indicates Progression in Advanced Glaucoma. *Ophthalmology* 2017;124:1466–74. [PubMed: 28549518]
28. Inuzuka H, Sawada A, Inuzuka M, Yamamoto T. Thinning rates of retinal nerve layer and ganglion cell-inner plexiform layer in various stages of normal tension glaucoma. *Br J Ophthalmol* 2020;104:1131–6. [PubMed: 31619379]
29. Hood DC, Kardon RH. A framework for comparing structural and functional measures of glaucomatous damage. *Prog Retin Eye Res* 2007;26:688–710. [PubMed: 17889587]

30. Rao HL, Pradhan ZS, Weinreb RN, et al. A comparison of the diagnostic ability of vessel density and structural measurements of optical coherence tomography in primary open angle glaucoma. *PLoS One* 2017;12:e0173930. [PubMed: 28288185]
31. Suda K, Hangai M, Akagi T, et al. Comparison of Longitudinal Changes in Functional and Structural Measures for Evaluating Progression of Glaucomatous Optic Neuropathy. *Invest Ophthalmol Vis Sci* 2015;56:5477–84. [PubMed: 26284553]
32. Leung CKS, Ye C, Weinreb RN, et al. Impact of age-related change of retinal nerve fiber layer and macular thicknesses on evaluation of glaucoma progression. *Ophthalmology* 2013;120:2485–92. [PubMed: 23993360]
33. Zhang X, Dastiridou A, Francis BA, et al. Comparison of Glaucoma Progression Detection by Optical Coherence Tomography and Visual Field. *Am J Ophthalmol* 2017;184:63–74. [PubMed: 28964806]
34. Lee WJ, Kim YK, Park KH, Jeoung JW. Trend-based Analysis of Ganglion Cell-Inner Plexiform Layer Thickness Changes on Optical Coherence Tomography in Glaucoma Progression. *Ophthalmology* 2017;124:1383–91. [PubMed: 28412067]
35. Hou HW, Lin C, Leung CK. Integrating Macular Ganglion Cell Inner Plexiform Layer and Parapapillary Retinal Nerve Fiber Layer Measurements to Detect Glaucoma Progression. *Ophthalmology* 2018;125:822–31. [PubMed: 29433852]
36. Shin JW, Sung KR, Song MK. Ganglion Cell-Inner Plexiform Layer and Retinal Nerve Fiber Layer Changes in Glaucoma Suspects Enable Prediction of Glaucoma Development. *Am J Ophthalmol* 2020;210:26–34. [PubMed: 31715157]
37. Nouri-Mahdavi K, Mohammadzadeh V, Rabiolo A, et al. Prediction of Visual Field Progression from OCT Structural Measures in Moderate to Advanced Glaucoma. *Am J Ophthalmol* 2021;226:172–81. [PubMed: 33529590]
38. Shin JW, Sung KR, Park SW. Patterns of Progressive Ganglion Cell-Inner Plexiform Layer Thinning in Glaucoma Detected by OCT. *Ophthalmology* 2018;125:1515–25. [PubMed: 29705057]
39. De Moraes CG, Juthani VJ, Liebmann JM, et al. Risk factors for visual field progression in treated glaucoma. *Arch Ophthalmol* 2011;129:562–8. [PubMed: 21555607]
40. Leske MC, Heijl A, Hussein M, et al. Factors for glaucoma progression and the effect of treatment: the early manifest glaucoma trial. *Arch Ophthalmol* 2003;121:48–56. [PubMed: 12523884]
41. Chan TCW, Bala C, Siu A, et al. Risk Factors for Rapid Glaucoma Disease Progression. *Am J Ophthalmol* 2017;180:151–7. [PubMed: 28624324]
42. Kim JH, Rabiolo A, Morales E, et al. Risk Factors for Fast Visual Field Progression in Glaucoma. *Am J Ophthalmol* 2019;207:268–78. [PubMed: 31238025]
43. Jammal AA, Berchuck SI, Thompson AC, et al. The Effect of Age on Increasing Susceptibility to Retinal Nerve Fiber Layer Loss in Glaucoma. *Invest Ophthalmol Vis Sci* 2020;61:8.
44. Budenz DL, Anderson DR, Feuer WJ, et al. Detection and prognostic significance of optic disc hemorrhages during the Ocular Hypertension Treatment Study. *Ophthalmology* 2006;113:2137–43. [PubMed: 16996592]
45. Bengtsson B, Leske MC, Yang Z, et al. Disc hemorrhages and treatment in the early manifest glaucoma trial. *Ophthalmology* 2008;115:2044–8. [PubMed: 18692244]
46. Founti P, Bunce C, Khawaja AP, et al. Risk Factors for Visual Field Deterioration in the United Kingdom Glaucoma Treatment Study. *Ophthalmology* 2020;127:1642–51. [PubMed: 32540325]
47. Diniz-Filho A, Abe RY, Zangwill LM, et al. Association between Intraocular Pressure and Rates of Retinal Nerve Fiber Layer Loss Measured by Optical Coherence Tomography. *Ophthalmology* 2016;123:2058–65. [PubMed: 27554036]
48. Jammal AA, Thompson AC, Mariottoni EB, et al. Impact of Intraocular Pressure Control on Rates of Retinal Nerve Fiber Layer Loss in a Large Clinical Population. *Ophthalmology* 2021;128:48–57. [PubMed: 32579892]

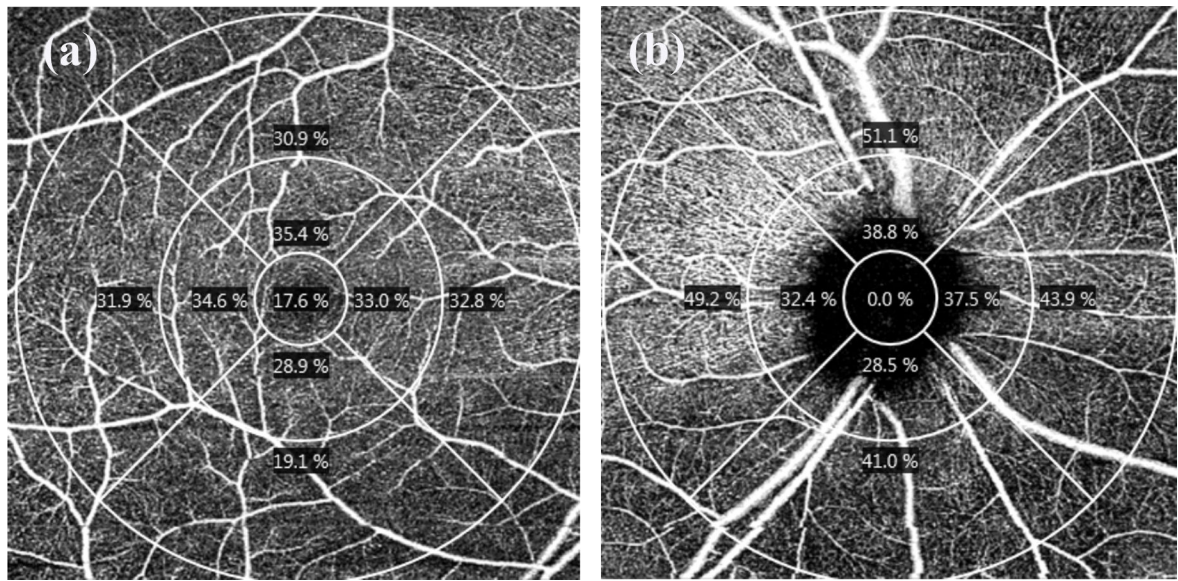


**Figure 1.**

Optical microangiography scans of the macula (a) and optic disc (b) showing the superficial layer vasculature in the right eye of a primary open-angle glaucoma patient. The images also show the Early Treatment Diabetic Retinopathy Study (ETDRS) grid centered on the macula and optic, and the perfusion density measurements calculated in each sector of the grid. In the current study, measurements from the superior and inferior outer quadrants (30.9% and 19.1% respectively in figure 1a and 51.1% and 41.0% respectively in figure 1b) of the scans were used for analysis.

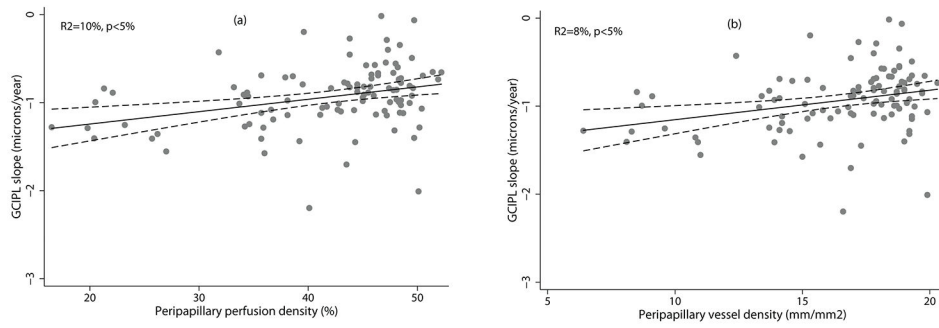


**Figure 2.** Scatterplots showing the relationship between rate of ganglion cell-inner plexiform layer (GCIPL) change and baseline peripapillary perfusion density (a), and peripapillary vessel density (b) of optical microangiography scan. R2 represents the coefficient of determination of the relationship.

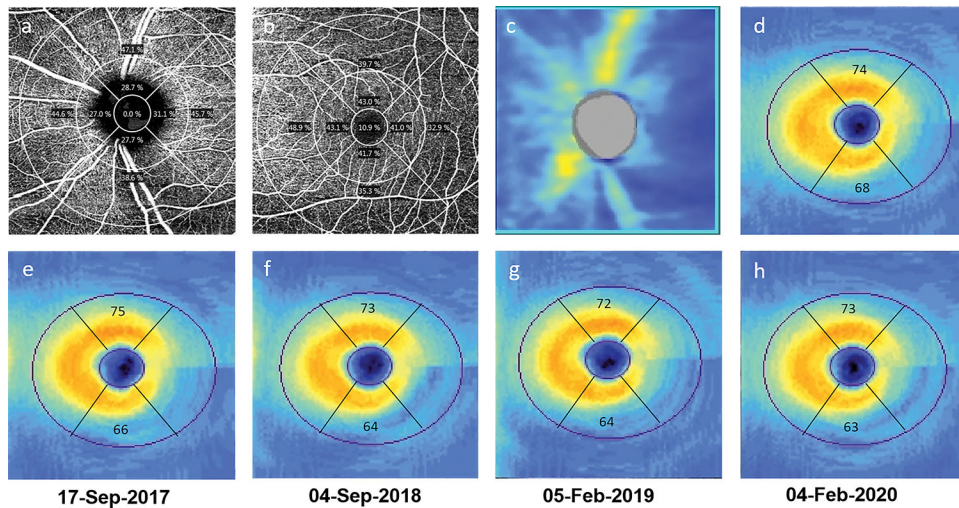


**Figure 3.** Example of a glaucomatous eye showing baseline peripapillary and macular optical microangiography (a and b) and optical coherence tomography scans (c and d) obtained on 07-September-2016. Peripapillary retinal nerve fiber layer scan (figure 3c) shows thinning in both superior and inferior quadrants. Figure 3d also shows the superior and inferior 60-degree sectors along which the ganglion cell-inner plexiform layer (GCIPL) thickness was measured (74 and 68 microns respectively) in the current study. Figures e-h show the follow-up scans along with the follow-up dates and the GCIPL thickness measurements in the superior and inferior sectors. Over a follow-up of approximately 3.5 years, GCIPL thickness in the superior sector remained stable while that in the inferior sector reduced from 68 microns to 63 microns.

**Table 1.**

Clinical features, visual field parameters and optical coherence tomography (OCT) measurements of the patients with primary open angle glaucoma (106 quadrants from 63 eyes of 38 patients).

	Mean $\pm$ SD	Range
Age (years)	59.6 $\pm$ 11.4	40 to 82
Gender (male:female)	31:7	
Hypertension (n, %)	15 (39.5%)	
Diabetes mellitus (n, %)	16 (42.1%)	
Spherical equivalent (diopter)	-0.4 $\pm$ 1.7	-5 to +2.5
Central corneal thickness ( $\mu$ m)	534 $\pm$ 36	451 to 598
No. of glaucoma medications at OCTA visit	1.1 $\pm$ 0.6	0 to 4
Hemifield (superior : Inferior)	55:51	
Baseline hemifield mean deviation (dB)	-5.2 $\pm$ 2.8	-11.9 to -0.2
Baseline quadrant RNFL thickness ( $\mu$ m)	94.5 $\pm$ 20.0	44 to 135
Baseline sector GCIPL thickness ( $\mu$ m)	72.4 $\pm$ 8.7	49 to 89
Baseline quadrant OCTA measurements		
Peripapillary perfusion density (%)	43.1 $\pm$ 7.0	19.8 to 52.2
Peripapillary vessel density (mm/mm <sup>2</sup> )	17.0 $\pm$ 2.6	8.3 to 20.3
Macular perfusion density (%)	37.2 $\pm$ 6.9	18.6 to 50.5
Macular vessel density (mm/mm <sup>2</sup> )	15.1 $\pm$ 2.6	7.9 to 19.5
Intraocular pressure (IOP) measurements		
Mean IOP during follow-up (mm Hg)	15.6 $\pm$ 2.8	10.7 to 23.8
IOP Fluctuation (SD) during follow-up (mm Hg)	2.5 $\pm$ 1.8	0.5 to 10.1
Disc hemorrhage during follow-up (n, %)	6 (5.7%)	
Follow-up duration (years)	3.0 $\pm$ 0.8	2.1 to 5.0
GCIPL slope ( $\mu$ m/year)	-0.97 $\pm$ 0.15	-1.3 to -0.7

dB: decibel; OCTA: optical coherence tomography angiography; RNFL: retinal nerve fiber layer; GCIPL: ganglion cell inner plexiform layer.



**Table 2.**

Results of univariate analysis evaluating the effect of each predictive variable on ganglion cell-inner plexiform layer (GCIPL) thickness measurement at baseline and progressive GCIPL change over time (slope) in primary open angle glaucoma eyes

	Effect on baseline GCIPL thickness		Effect on GCIPL Slope	
	Coefficient ± SE	P	Coefficient ± SE	P
Age	0.01 ± 0.10	0.91	-0.03 ± 0.01	0.02
Gender (Female as ref)	-0.80 ± 3.10	0.80	0.77 ± 0.40	0.05
Hypertension	-3.05 ± 2.34	0.19	-0.15 ± 0.31	0.63
Diabetes Mellitus	-0.86 ± 2.36	0.71	-0.27 ± 0.30	0.38
Spherical equivalent	1.62 ± 0.54	0.003	-0.04 ± 0.07	0.62
Central corneal thickness	-0.06 ± 0.04	0.09	0.004 ± 0.01	0.43
Mean deviation	0.57 ± 0.26	0.03	-0.004 ± 0.04	0.93
Baseline RNFL thickness	0.27 ± 0.03	<0.001	-0.01 ± 0.01	0.28
Baseline GCIPL thickness	0.99 ± 0.02	<0.001	-0.01 ± 0.02	0.70
Peripapillary perfusion density	0.42 ± 0.11	<0.001	0.04 ± 0.02	0.01
Peripapillary vessel density	1.16 ± 0.29	<0.001	0.09 ± 0.04	0.04
Macular perfusion density	0.45 ± 0.11	<0.001	0.02 ± 0.02	0.25
Macular vessel density	1.27 ± 0.28	<0.001	0.05 ± 0.05	0.20
Mean IOP during follow-up	-0.65 ± 0.39	0.09	0.01 ± 0.05	0.90
IOP SD during follow-up	-0.79 ± 0.59	0.18	0.07 ± 0.08	0.41
Presence of disc hemorrhage	-3.69 ± 2.88	0.20	-0.93 ± 0.42	0.03
Signal strength of GCIPL scans	0.05 ± 0.28	0.84	0.04 ± 0.15	0.80

SE: standard error; RNFL: retinal nerve fiber layer; IOP: intraocular pressure; SD: standard deviation.

**Table 3.**

Results of multivariate mixed effect models showing the factors associated with the slope of ganglion cell-inner plexiform layer thickness in primary open angle glaucoma eyes

	Model 1		Model 2	
	Coefficient $\pm$ SE	P	Coefficient $\pm$ SE	P
Age	-0.03 $\pm$ 0.01	0.007	-0.03 $\pm$ 0.01	0.006
Gender (Female as ref)	0.34 $\pm$ 0.33	0.31	0.31 $\pm$ 0.34	0.36
Presence of disc hemorrhage	-0.09 $\pm$ 0.29	0.76	-0.09 $\pm$ 0.29	0.76
Peripapillary perfusion density	0.04 $\pm$ 0.02	0.01		
Peripapillary vessel density			0.09 $\pm$ 0.04	0.05

SE: standard error.

Author Manuscript

Author Manuscript

Author Manuscript

Author Manuscript